Scientia Iranica B (2023) 30(1), 16–29

Sharif University of Technology
Scientia Iranica
Transactions B: Mechanical Engineering
http://scientiairanica.sharif.edu

Position synchronization for an uncertain teleoperation system with time delays using L_1 theory

B. Yazdankhoo[a], F. Najafi[a,*], M.R. Ha´iri Yazdi[a,c], and B. Beigzadeh[b]

a. *School of Mechanical Engineering, College of Engineering, University of Tehran, Tehran, P.O. Box 1439957131, Iran.*
b. *Biomechatronics and Cognitive Engineering Research Lab, School of Mechanical Engineering, Iran University of Science and Technology, Tehran, P.O. Box 16765163, Iran.*
c. *Department of Mechanical Engineering, Lassonde School of Engineering, York University, Toronto, Canada.*

Received 22 October 2021; received in revised form 6 May 2022; accepted 28 November 2022

KEYWORDS
Teleoperation;
L_1 theory;
State-feedback controller;
Time delay;
Linear Matrix Inequality (LMI);
Sliding mode controller.

Abstract. The problem of position tracking in teleoperation systems equipped with latencies and dynamical uncertainties was addressed in this study. In many applications, such as telesurgery, safe interaction with the external environment is a factor that may undermine the synchronization of the positions. In the case of nondestructive contact with the environment, in addition to an errorless steady-state position tracking, the closed-loop system requires a response with the least possible overshoot. To this end, a state-feedback controller based upon L_1 theory was proposed in this paper. The compensator was synthesized using Linear Matrix Inequality (LMI) technology, and the asymptotic stability of the system was verified through Lyapunov-Krasovskii functional. Considered its advantage, the proposed control scheme is robust to asymmetric randomly varying time delays in the communication channels. The L_1-based controller was finally compared to the well-known sliding mode controller through simulation, and it proved to outperform its counterpart from the maximum error point of view while preserving low steady-state error. The proposed controller was also proved to be effective even in the presence of model uncertainties.

1. Introduction

Control of teleoperation systems has always been a major challenge due to the existing latencies, packet loss, etc. imposed by communication channels. Although the recent advent of 5G network technology has led to a marked improvement, especially in time delay reduction [1]. This issue might not be conceived of as thoroughly mitigated since, for instance, communication with other planets is still subject to time delay.

*. *Corresponding author. Tel.: +1 778 782 7603*
E-mail address: farshid_najafi@sfu.ca (F. Najafi)

doi: 10.24200/sci.2022.59285.6158

Various methods have been proposed in the literature concerning how to control the delayed teleoperation systems [2]. The sliding mode control was proposed as a promising approach, especially when integrated with other methods such as impedance control for the purpose of force control [3] or when used as a means of disturbance rejection [4]. Adaptive control methods have also been widely used in teleoperation systems [5]. They have been applied both in the classical form, such as model-reference adaptive control [6], and in more modern forms in combination with other control approaches, such as passivity-based [7] and model predictive [8] control.

Predictive control has been another widely used approach in recent years [9]. It has been applied to both sides of a teleoperation system: to the operator side as model-mediated teleoperation [10] and to the teleoperator side to predict the human motion before/after transmitting it through communication channel, with either constant known time delays [11] or both constant and variable but unknown time delays [12].

Robust control is another approach that maintains its stability in the presence of uncertainties and external disturbances as well as acceptable tracking performance of the slave robot [13]. The most well-known robust method in the field of teleoperation is H_∞ theory [14]. Moreover, many recent researches such as [15] rely on Lyapunov-Krasovskii methods in order to robustify the system against the external disturbances.

The main focus of the aforementioned approaches is mainly dedicated to the steady-state behavior of the system, and the transient response is often overlooked. Transient behavior of a robotic system might be of great importance when it interacts with the external environments. For instance, excessive force imposed on or penetration into the body tissues in a robotic surgery system will definitely cause serious damages to them [16]. In the case of teleoperation, however, the significance of transient response becomes even more remarkable due to the encompassing time delays [17]. Therefore, possessing an overshoot-free position tracking, which is categorized as a transient characteristic, in a teleoperation system is highly indispensable.

Introduced by Vidyasagar in 1986 [18], L_1 theory is a robust approach that takes control of the amplitude, instead of the energy, of the response when system is subject to a bounded external disturbance. This provides us with a powerful tool that helps reach an optimized transient behavior. Another advantage of L_1 method is that it transfers the analysis of the system from frequency domain (which is the case for H_∞ theory) directly to the time domain [19]. Finally, L_1 control makes the system free of the condition of energy boundedness of the external disturbance.

Meanwhile, L_1 control of teleoperation systems faces a major challenge, i.e., a majority of the L_1-based compensators in previous works were designed for systems without any time delay. Nonetheless, there are very few research studies on the application of L_1 theory in time-delayed systems. For example, in [20], a small-gain theorem was developed for time-delayed systems based on L_1 theory, or in [21], L_1 filtering methods were proposed for systems with time delay. In addition, in [22], the design of a controller for systems with latency based on the optimal L_1 theory for linear parameter-varying systems was investigated. In [23], the very case for air heater systems was studied. Further, in [24], L_1 adaptive control for delayed systems was discussed.

To the authors' knowledge, no significant attention has been drawn to L_1 control of teleoperation systems yet. However, one research work previously proposed an L_1-based controller for a teleoperation system with varying time delays [25], in which the interaction between the teleoperator and the environment was ignored and the uncertainties of the robot were not included in the results. For this reason, the authors felt the need to focus on this research gap in this study.

It should also be noted that in many previously presented control frameworks for teleoperation systems, position tracking was achieved at the expense of degrading the haptic sensation of the operator [26]. In this paper, however, we intend to provide the operator with complete haptic feedback which, in turn, complicates the design procedure since manipulation of only one controller was freely allowed.

To sum up, the main objective of the current research is to design and control an uncertain teleoperation system with randomly varying latencies using L_1 theory in order to minimize the overshoot of the position tracking, without sacrificing the force transparency of the system. To this end, Linear Matrix Inequality (LMI) technique was employed. Our contribution in this paper includes designing a compensator for an uncertain teleoperation system, characterized by asymmetric randomly varying time delays and interaction with the external environment based on L_1 theory, which ensures prescribed overshoot, in addition to retaining an acceptable steady-state response and complete force feedback.

The rest of this paper is organized as follows. In Section 2, the problem is mathematically formulated, and the design criteria are determined. In Section 3, the steps toward the synthesis of the L_1 controller through LMIs are discussed. In Section 4, the efficacy of the proposed architecture is validated through simulation studies. Finally, in Section 5, concluding remarks and future suggestions are presented.

2. Problem formulation

The block diagram of the proposed teleoperation system in this paper is depicted in Figure 1. According to this figure, it consists of master and slave sides connected by communication channels. The master robot, denoted by G_m, constitutes the master side. The slave side is composed of the slave robot, controller, low-pass filter, and environment that are denoted by G_s, C_s, G_f, and Z_e, respectively. The communication channel comprises the forward and backward time delays, namely d_m and d_s.

The master and slave robots are considered to have a one-Degree-of-Freedom (one-DoF) linear second-order model, which is written in the following form:

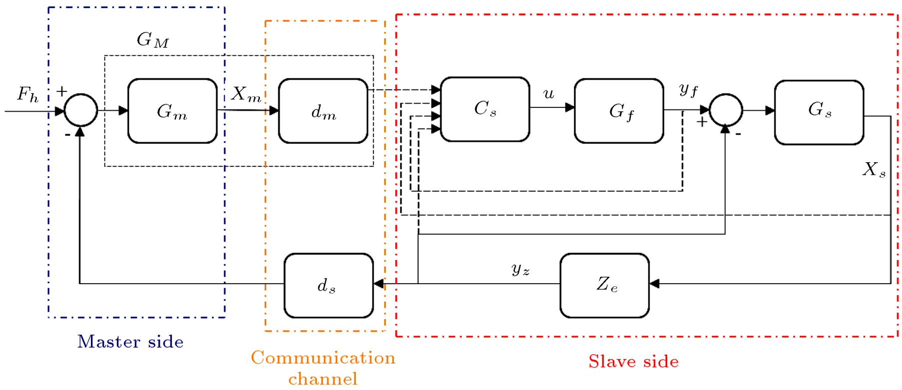

Figure 1. Proposed teleoperation architecture.

$$m_m(\rho)\ddot{x}_m(t) + b_m(\rho)\dot{x}_m(t) + k_m(\rho)x_m(t) = F_h(t) - y_z(t - d_s(t)), \tag{1}$$

$$m_s(\rho)\ddot{x}_s(t) + b_s(\rho)\dot{x}_s(t) + k_s(\rho)x_s(t) = y_f(t) - y_z(t), \tag{2}$$

where the system dynamics depend on ρ and contain uncertain parameters, which will be defined later in this section.

The state-space representation of the above equations is as follows:

$$G_m: \begin{cases} \dot{\mathbf{x}}_m(t) = A_m(\rho)\mathbf{x}_m(t) + B_m(\rho)\left(w(t) - y_z(t - d_s(t))\right) \\ y_m(t) = C_m\mathbf{x}_m(t) \end{cases} \tag{3}$$

$$G_s: \begin{cases} \dot{\mathbf{x}}_s(t) = A_s(\rho)\mathbf{x}_s(t) + B_s(\rho)\left(y_f(t) - y_z(t)\right) \\ y_s(t) = C_s\mathbf{x}_s(t) \end{cases} \tag{4}$$

where $\mathbf{x}_i \triangleq \begin{bmatrix} x_i^T & \dot{x}_i^T \end{bmatrix}^T$ and:

$$A_i(\rho) \triangleq \begin{bmatrix} 0 & 1 \\ -k_i(\rho)/m_i(\rho) & -b_i(\rho)/m_i(\rho) \end{bmatrix},$$

$$B_i(\rho) \triangleq \begin{bmatrix} 0 & 1/m_i(\rho) \end{bmatrix}^T, \; C_i \triangleq I_{2\times 2}.$$

In order to take the forward (master-to-slave) time delay $d_m(t)$ into account, it was combined with the dynamics of the master robot G_m to form a unified representation, as shown in Eq. (5):

$$G_M: \begin{cases} \dot{\bar{\mathbf{x}}}_m(t) = A_m(\rho)\bar{\mathbf{x}}_m(t) + B_m(\rho)\left(\bar{w}(t) - y_z(t - d(t))\right) \\ \bar{y}_m(t) = C_m\bar{\mathbf{x}}_m(t) \end{cases} \tag{5}$$

where $\bar{\mathbf{x}}_m(t) \triangleq \mathbf{x}_m(t - d_m(t))$, $\bar{w}(t) \triangleq w(t - d_m(t))$, $\bar{y}_m(t) \triangleq y_m(t - d_m(t))$, and $d(t) \triangleq d_m(t) + d_s(t)$ represent the aggregate of the forward and backward time delays in the communication channel, which will hereinafter be called Total Time Delay (TTD).

To prevent high-frequency oscillations in the control signal that causes damage to the actuator, a low-pass filter was placed after the controller, as shown in Figure 1. The filter is in the form of $G_f(s) = \frac{\omega_0}{s+\omega_0}$ where ω_0 is the cut-off frequency, which can be written in the state space notation as:

$$G_f: \begin{cases} \dot{x}_f(t) = A_f x_f(t) + B_f u(t) \\ y_f(t) = C_f x_f(t) \end{cases} \tag{6}$$

where $A_f \triangleq -\omega_0$, $B_f \triangleq \omega_0$, $C_f \triangleq 1$, and $u(t)$ are the control inputs. A general linear viscoelastic model was assumed for the environment which could be represented in Eq. (7):

$$Z_e: \; y_z(t) = D_z(\rho)y_s(t), \tag{7}$$

where $D_z(\rho) \triangleq \begin{bmatrix} k_z(\rho) & b_z(\rho) \end{bmatrix}$ denote the vector of the stiffness and damping coefficient of the environment. Upon substituting the output Eq. (4) into Eq. (7), we have:

$$y_z(t) = D_z(\rho)C_s\mathbf{x}_s(t). \tag{8}$$

The error of the system is defined as follows:

$$x_e(t) \triangleq \int_0^t e(\xi)\, d\xi, \tag{9}$$

where $e(t) \triangleq \bar{x}_m(t) - x_s(t)$ is the position error. Therefore, the error dynamics is obtained as follows:

$$\dot{x}_e(t) = C_{1e}\bar{\mathbf{x}}_m(t) + C_{2e}\mathbf{x}_s(t), \tag{10}$$

where $C_{1e} \triangleq \begin{bmatrix} 1 & 0 \end{bmatrix}$ and $C_{2e} \triangleq \begin{bmatrix} -1 & 0 \end{bmatrix}$. Next, by combining Eqs. (4), (5), (8), and (10), the open-loop system can be written by Eq. (11) as shown in Box I, where $\mathbf{x}(t) \triangleq \begin{bmatrix} \bar{\mathbf{x}}_m^T(t) & \mathbf{x}_s^T(t) & x_f^T(t) & x_e^T(t) \end{bmatrix}^T$ is the system state vector.

In this paper, a state-feedback controller was used for the teleoperation system. Hence, the control signal can be formulated as:

$$u(t) = K\mathbf{x}(t), \tag{12}$$

$$G_{ol}: A(\rho)\mathbf{x}(t) + A_d(\rho)\mathbf{x}(t-d(t)) + B_1(\rho)\bar{w}(t) + B_2 u(t)$$

$$A(\rho) \triangleq \begin{bmatrix} A_m(\rho) & 0 & 0 & 0 \\ 0 & A_s(\rho) - B_s(\rho)D_z(\rho)C_s & B_s(\rho)C_f & 0 \\ 0 & 0 & A_f & 0 \\ C_{1e} & C_{2e} & 0 & 0 \end{bmatrix},$$

$$A_d(\rho) \triangleq \begin{bmatrix} 0 & -B_m(\rho)D_z(\rho)C_s & 0 & 0 \\ 0 & 0 & 0 & 0 \\ 0 & 0 & 0 & 0 \\ 0 & 0 & 0 & 0 \end{bmatrix}, \tag{11}$$

$$B_1(\rho) \triangleq \begin{bmatrix} B_m^T(\rho) & 0 & 0 & 0 \end{bmatrix}^T, \; B_2 \triangleq \begin{bmatrix} 0 & 0 & B_f^T & 0 \end{bmatrix}^T.$$

Box I

where K denotes the control gain matrix. Now, based on Eqs. (11) and (12), the uncertain closed-loop system can be obtained as:

$$G_{cl}: \begin{cases} \dot{\mathbf{x}}(t) = \bar{A}(\rho)\mathbf{x}(t) + A_d(\rho)\mathbf{x}(t-d(t)) + B_1(\rho)\bar{w}(t) \\ z(t) = C\mathbf{x}(t) \end{cases}$$
$$\bar{A}(\rho) \triangleq A(\rho) + B_2 K \tag{13}$$

where $C = \begin{bmatrix} 0 & 0 & 0 & 1 \end{bmatrix}$ and $z(t)$ are the L_1 performance variables. The closed-loop system matrices possess uncertain dynamics, which are considered to be encompassed by a polytope with n vertices:

$$\omega^{(k)} \triangleq \left(A^{(k)}, A_d^{(k)}, B_1^{(k)}\right) \in \Omega, \quad k = 1, ..., n, \tag{14}$$

where Ω is the convex hull of the vertices constituting the polyhedral domain of uncertainty, which can be defined as:

$$\Omega \triangleq \{\mathcal{H}(\rho) | \rho = (\rho_1, ..., \rho_n)\}, \tag{15}$$

$$\mathcal{H}(\rho) \triangleq \left\{\sum_{k=1}^{n} \rho_k \omega^{(k)} | \rho_k \geq 0, \;\; k = 1, ..., n; \;\; \sum_{k=1}^{n} \rho_k = 1\right\}. \tag{16}$$

The TTD of the system should satisfy the following criteria:

$$0 \leq d(t) \leq \tilde{d} < \infty, \;\; |\dot{d}(t)| \leq \tilde{\tau} < 1; \;\; \forall t \geq 0. \tag{17}$$

The lower bound for the derivative of the TTD stems from the fact that the order of the data packets must not be changed when transmitted through the communication channels.

Now, given the close-loop system G_{cl} in Eq. (13), the objective here is to find the controller gain matrix K based on the L_∞-induced norm of the system such that:

- G_{cl} is asymptotically stable.
- G_{cl} guarantees the prescribed L_1 performance:

$$||T_{zw}||_1 \triangleq \sup_{w(t)\neq 0} \frac{||z(t)||_\infty}{||w(t)||_\infty} < \gamma,$$

under zero initial conditions, where T_{zw} represents the convolutional operator from the disturbance $w(t) \in L_\infty[0, \infty)$ to the performance output $z(t)$, and $\gamma \in \mathbb{R}^+$ is the noise attenuation level.

Note that the infinity-norm of an arbitrary signal $||f(t)||_\infty$ is defined as $\left(\sup_t f^T(t)f(t)\right)^{\frac{1}{2}}$.

3. Synthesis of L_1-based controller

In this section, a controller for the teleoperation system is designed through three parts, the first of which is elaborated below.

Theorem 1. The closed-loop system G_{cl} in Eq. (13) is asymptotically stable which guarantees the L_1 performance criterion (i.e., has the noise attenuation level γ) if there exist a scalar $\alpha > 0$ and matrices $P(\rho) > 0$, $Q(\rho) > 0$, and $R(\rho) > 0$ with appropriate dimensions satisfying:

Eq. (18) is shown in Box II.

$$\alpha Q(\rho) - (1 - \alpha\tilde{d})R(\rho) < 0, \tag{19}$$

$$\begin{bmatrix} -\alpha P(\rho) & 0 & C^T \\ * & -(\gamma - \alpha)I & 0 \\ * & * & -\gamma I \end{bmatrix} < 0, \tag{20}$$

where * denotes the symmetric terms.

$$\begin{bmatrix} \begin{matrix} \bar{A}^T(\rho)P(\rho) + P(\rho)\bar{A}(\rho) \\ +\alpha P(\rho) + Q(\rho) + \tilde{d}R(\rho) \end{matrix} & P(\rho)A_d(\rho) & P(\rho)B_1(\rho) \\ * & -(1-\tilde{\tau})Q(\rho) & 0 \\ * & * & -\alpha I \end{bmatrix} < 0. \tag{18}$$

Box II

Proof. For every fixed $\rho \in \Omega$, the Lyapunov-Krasovskii functional is chosen as:

$$V(\mathbf{x}(t)) = \mathbf{x}^T(t)P\mathbf{x}(t) + \int_{t-d(t)}^{t} \mathbf{x}^T(\xi)Q\mathbf{x}(\xi)d\xi + \int_{t-\tilde{d}}^{t}\int_{\xi}^{t} \mathbf{x}^T(\varepsilon)R\mathbf{x}(\varepsilon)d\varepsilon d\xi, \tag{21}$$

where $P > 0$, $Q > 0$, $R > 0$ are the matrices to be determined. Taking the time derivative of Eq. (21) leads to:

$$\dot{V} = \mathbf{x}^T(t)\left(\bar{A}^TP + P\bar{A} + Q\right)\mathbf{x}(t) + 2\mathbf{x}^T(t)PB_1\bar{w}(t) + 2\mathbf{x}^T(t-d(t)){A_d}^TP\mathbf{x}(t) - \left\{1 - \frac{\partial}{\partial t}(d(t))\right\} \mathbf{x}^T(t-d(t))Q\mathbf{x}(t-d(t)) + \tilde{d}\mathbf{x}^T(t)R\mathbf{x}(t) - \int_{t-\tilde{d}}^{t} \mathbf{x}^T(\xi)R\mathbf{x}(\xi)d\xi. \tag{22}$$

Now, by defining:

$$\Phi(t) \triangleq \begin{bmatrix} \mathbf{x}^T(t) & \mathbf{x}^T(t-d(t)) & \bar{w}^T(t) \end{bmatrix}^T,$$

one can write Eq. (23) as shown in Box III. Equivalently, Inequality (23) might be written by Eq. (24) as shown in Box IV.

In the following, three inequalities derived from some ordinary manipulations are shown. First, we can write Eq. (25) as shown in Box V. If Inequality (19) holds, we will have:

$$\int_{t-\tilde{d}}^{t}\int_{\xi}^{t} \mathbf{x}^T(\varepsilon)\left(R - \alpha Q\right)\mathbf{x}(\varepsilon)d\varepsilon d\xi < \tilde{d}\int_{t-\tilde{d}}^{t} \mathbf{x}^T(\xi)\left(R - \alpha Q\right)\mathbf{x}(\xi)d\xi, \tag{26}$$

$$\alpha\tilde{d}R < R - \alpha Q. \tag{27}$$

Therefore, we have:

$$\dot{V} < \Phi^T(t)\Delta'\Phi(t) + \alpha\bar{w}^T(t)\bar{w}(t) - \alpha\int_{t-d(t)}^{t} \mathbf{x}^T(\xi)Q\mathbf{x}(\xi)d\xi - \alpha\int_{t-\tilde{d}}^{t}\int_{\xi}^{t} \mathbf{x}^T(\varepsilon)R\mathbf{x}(\varepsilon)d\varepsilon d\xi - \alpha\mathbf{x}^T(t)P\mathbf{x}(t) = \Phi^T(t)\Delta'\Phi(t) + \alpha\bar{w}^T(t)\bar{w}(t) - \alpha V, \tag{28}$$

$$\dot{V} \le \Phi^T(t)\Xi\Phi(t) + \alpha\bar{w}^T(t)\bar{w}(t) - \alpha\int_{t-d(t)}^{t} \mathbf{x}^T(\xi)Q\mathbf{x}(\xi)d\xi - \int_{t-\tilde{d}}^{t} \mathbf{x}^T(\xi)\left(R - \alpha Q\right)\mathbf{x}(\xi)d\xi\Xi \triangleq \begin{bmatrix} \bar{A}^TP + P\bar{A} + Q + \tilde{d}R & PA_d & PB_1 \\ * & -\left[1 - \frac{\partial}{\partial t}(d(t))\right]Q & 0 \\ * & * & -\alpha I \end{bmatrix}. \tag{23}$$

Box III

$$\dot{V} \le \Phi^T(t)\Delta\Phi(t) + \alpha\bar{w}^T(t)\bar{w}(t) - \alpha\int_{t-d(t)}^{t} \mathbf{x}^T(\xi)Q\mathbf{x}(\xi)d\xi - \int_{t-\tilde{d}}^{t} \mathbf{x}^T(\xi)\left(R - \alpha Q\right)\mathbf{x}(\xi)d\xi - \alpha\mathbf{x}^T(t)P\mathbf{x}(t)\Delta \triangleq \begin{bmatrix} \bar{A}^TP + P\bar{A} + Q + \tilde{d}R + \alpha P & PA_d & PB_1 \\ * & -\left[1 - \frac{\partial}{\partial t}(d(t))\right]Q & 0 \\ * & * & -\alpha I \end{bmatrix}. \tag{24}$$

Box IV

$$\Phi^T(t)\Delta\Phi(t) \leq \Phi^T(t)\Delta'\Phi(t)\Delta' \triangleq \begin{bmatrix} \bar{A}^T P + P\bar{A} + Q + \tilde{d}R + \alpha P & PA_d & PB_1 \\ * & -(1-\tilde{\tau})Q & 0 \\ * & * & -\alpha I \end{bmatrix}. \quad (25)$$

Box V

$\Delta' < 0$ (which is exactly same as Inequality (18) for every $\rho \in \Omega$) guarantees that $\Phi^T(t)\Delta'\Phi(t) < 0$. Consequently, the problem can now be reduced to as follows:

$$\dot{V} < \alpha\bar{w}^T(t)\bar{w}(t) - \alpha V. \quad (29)$$

For $\forall\,\Phi(t) \neq 0$ and $\forall\,\bar{w}(t) = 0$, Inequality (29) results in $\dot{V} < 0$, which proves the asymptotic stability of G_{cl}.

The L_1 performance satisfaction is now discussed. In case we consider Inequality (29) in $\forall\bar{w}(t) \neq 0$, we will have two possible conditions. If $\dot{V} \geq 0$, $V \leq \bar{w}^T(t)\bar{w}(t)$ for $\forall t \geq 0$. On the contrary, if $\dot{V} < 0$, the right-hand side term of Inequality (29) can become either positive or negative. It should also be noted that $\alpha\bar{w}^T(t)\bar{w}(t) - \alpha V \geq 0$ yields the previous result. However, $\alpha\bar{w}^T(t)\bar{w}(t) - \alpha V < 0$ leads to $\bar{w}^T(t)\bar{w}(t) < V$, which is a contradiction since initially $V(\mathbf{x}(0)) = 0$, as per the assumption of zero initial conditions and consequently, V will never exceed $\bar{w}^T(t)\bar{w}(t)$ for $\forall t > 0$, regardless of the sign of $\dot{V}$.

Consequently, we always have $0 \leq V \leq \bar{w}^T(t)\bar{w}(t)$ and thus $0 \leq \mathbf{x}^T(t)P\mathbf{x}(t) \leq \bar{w}^T(t)\bar{w}(t)$. Now if the following inequality holds:

$$\frac{1}{\gamma}z^T(t)z(t) - \alpha\mathbf{x}^T(t)P\mathbf{x}(t) - (\gamma-\alpha)\bar{w}^T(t)\bar{w}(t) < 0, \quad (30)$$

the condition $z^T(t)z(t) < \gamma^2\bar{w}^T(t)\bar{w}(t)$ will clearly be concluded. Rewriting Inequality (30) in the form of:

$$\begin{bmatrix} \mathbf{x}^T(t) & \bar{w}^T(t) \end{bmatrix} \begin{bmatrix} -\alpha P + \frac{1}{\gamma}C^T C & 0 \\ * & -(\gamma-\alpha)I \end{bmatrix} \begin{bmatrix} \mathbf{x}(t) \\ \bar{w}(t) \end{bmatrix} < 0, \quad (31)$$

and further applying Schur complement lead to Inequality (20) for every $\rho \in \Omega$. Therefore, it can be conveniently concluded that:

$$\sup_{w(t)\neq 0} \frac{||z(t)||_\infty}{||w(t)||_\infty} < \gamma, \quad \forall t \geq 0. \quad (32)$$

Hence, the L_1 condition is fulfilled and the proof is completed. □

Remark 1. If α is held constant, Conditions (18), (19), and (20) are LMIs and thus, the problem is converted into an optimization problem; hence, we have:

$$\min_{\mathcal{S}} \gamma \text{ s.t. } (18), (19), (20), \quad (33)$$

where $\mathcal{S} \triangleq \{\alpha,\ P(\rho),\ Q(\rho),\ R(\rho)\}$. In addition, the following inequality for α must be satisfied in order for Inequality (18) to yield a positive definite solution [21]:

$$0 < \alpha < -2\max\left\{\mathrm{Re}\left[\lambda\left(\bar{A}(\rho)\right)\right]\right\}, \quad (34)$$

where $\lambda(.)$ represents the eigenvalue.

Remark 2. Since $\bar{A}(\rho)$ depends on the controller gain matrix K, Inequality (34) imposes a condition on α which is a beneficial tool for validating the resulting α after obtaining the controller. It, however, does not set any condition on the domain of α to be used prior to designing the controller. Nevertheless, if Inequality (19) is to result in a positive definite solution, $\alpha\tilde{d} < 1$ must be satisfied. Hence, one can set $0 < \alpha < \frac{1}{\tilde{d}}$ as the domain of search for the aforementioned optimization problem.

Remark 3. Theorem 1 states the conditions for the closed-loop system to meet the design criteria; however, it will not lead to the design of the controller due to the presence of $\bar{A}(\rho)$ in Inequality (18). Therefore, the remaining two parts of the controller design aim to build an algorithm for the desired controller design. The second part is stated by the following theorem.

Theorem 2. The closed-loop system G_{cl} in Eq. (13) is asymptotically stable that guarantees the L_1 performance criterion (i.e., with the noise attenuation level of γ), if there exist a scalar $\alpha > 0$ and matrices $P(\rho) > 0$, $Q(\rho) > 0$, $R(\rho) > 0$, and $W(\rho)$ with appropriate dimensions satisfying Inequalities (18), (19) and (35):

$$\begin{bmatrix} \Gamma_{11}(\rho) & \Gamma_{12}(\rho) \\ * & \Gamma_{22}(\rho) \end{bmatrix} < 0. \quad (35)$$

$\Gamma_{11}(\rho)$ is calculated by the equation shown in Box VI and $\Gamma_{12}(\rho)$ and $\Gamma_{22}(\rho)$ are calculated by the following equations:

$$\Gamma_{12}(\rho) \triangleq \begin{bmatrix} W^T(\rho)\bar{A}_d(\rho) & W^T(\rho)B_1(\rho) & W^T(\rho) \\ 0 & 0 & 0 \end{bmatrix},$$

$$\Gamma_{11}(\rho) \triangleq \begin{bmatrix} -(W(\rho)+W^T(\rho)) & P(\rho)+W^T(\rho)\bar{A}(\rho) \\ * & -P(\rho)+\alpha P(\rho)+Q(\rho)+\tilde{d}R(\rho) \end{bmatrix}.$$

Box VI

$$\Gamma_{22}(\rho) \triangleq diag\{\ -(1-\tilde{\tau})Q(\rho),\quad -\alpha I,\quad -P(\rho)\ \}.$$

Proof. The proof could be easily concluded from Theorem 2 of [22], putting matrix Z therein equal to zero and omitting its respective rows and/or columns in each matrix. □

Finally, the third part of the L_1 controller synthesis is as follows:

Theorem 3. The closed-loop system G_{cl} in Eq. (13) is asymptotically stable and guarantees the L_1 performance criterion (i.e., with the noise attenuation level of γ), if there exist a scalar $\alpha>0$ and matrices $P'(\rho)>0$, $Q'(\rho)>0$, $R'(\rho)>0$, $G(\rho)$, and $M(\rho)$ with appropriate dimensions satisfying:

Inequality (36) is shown in Box VII,

$$\alpha Q'(\rho)-(1-\alpha\tilde{d})R'(\rho)<0, \tag{37}$$

$$\begin{bmatrix} -\alpha P'(\rho) & 0 & G^T(\rho)C^T \\ * & -(\gamma-\alpha)I & 0 \\ * & * & -\gamma I \end{bmatrix}<0. \tag{38}$$

Further, the desired controller can be obtained as follows:

$$K(\rho)=M(\rho)G^{-1}(\rho). \tag{39}$$

Proof. Similar to the procedure in [22], first, the following matrices are defined as follows:

$$G(\rho)\triangleq W^{-1}(\rho),$$

$$P'(\rho)\triangleq W^{-T}(\rho)P(\rho)W^{-1}(\rho),$$

$$Q'(\rho)\triangleq W^{-T}(\rho)Q(\rho)W^{-1}(\rho),$$

$$R'(\rho)\triangleq W^{-T}(\rho)R(\rho)W^{-1}(\rho). \tag{40}$$

Then, by applying congruence transformations to Inequalities (35), (19), and (20) by $diag\{W^{-1}(\rho),\ \ W^{-1}(\rho),\ \ W^{-1}(\rho),\ \ I,\ \ W^{-1}(\rho)\}$, $W^{-1}(\rho)$, and $diag\{W^{-1}(\rho),\ \ I,\ \ I\}$, respectively, we can obtain Inequalities (36)–(38) and the controller gain (Eq. (39)). □

Remark 4. One problem that arises from applying Theorem 3 to the L_1 controller design is that due to the dependence of the LMIs on ρ, infinite sets of LMIs should be solved to cover the whole uncertainty domain Ω. However, by adopting the concept of quadratic stability, the problem can be narrowed down to the finite set of LMIs. This fact is reflected in the following corollary from Theorem 3.

Corollary 1. The closed-loop system G_{cl} in Eq. (13) is asymptotically stable and ensures the L_1 performance criterion (i.e., with the noise attenuation level of γ) if there exist a scalar $\alpha>0$ and matrices $P'>0$, $Q'>0$, $R'>0$, G, and M with appropriate dimensions that satisfy:

Inequality (41) is shown in Box VIII,

$$\alpha Q'-(1-\alpha\tilde{d})R'<0, \tag{42}$$

$$\begin{bmatrix} -\alpha P' & 0 & G^TC^T \\ * & -(\gamma-\alpha)I & 0 \\ * & * & -\gamma I \end{bmatrix}<0, \tag{43}$$

for $k=1,...,n$.

Proof. According to the concept of quadratic stability, the matrices $P'(\rho)=P'$, $Q'(\rho)=Q'$, $R'(\rho)=R'$, $G(\rho)=G$, and $M(\rho)=M$ are all held fixed throughout the entire uncertainty domain Ω. In addition, since

$$\begin{bmatrix} -G^T(\rho)-G(\rho) & \begin{matrix} P'(\rho)+A(\rho)G(\rho) \\ +B_2M(\rho) \end{matrix} & A_d(\rho)G(\rho) & B_1(\rho) & G(\rho) \\ * & \begin{matrix} -P'(\rho)+\alpha P'(\rho) \\ +Q'(\rho)+\tilde{d}R'(\rho) \end{matrix} & 0 & 0 & 0 \\ * & * & -(1-\tilde{\tau})Q'(\rho) & 0 & 0 \\ * & * & * & -\alpha I & 0 \\ * & * & * & * & -P'(\rho) \end{bmatrix}<0. \tag{36}$$

Box VII

$$\begin{bmatrix} -G^T - G & P' + A^{(k)}G + B_2 M & A_d^{(k)} G & B_1^{(k)} & G \\ * & -P' + \alpha P' + Q' + \tilde{d} R' & 0 & 0 & 0 \\ * & * & -(1-\tilde{\tau})\, Q' & 0 & 0 \\ * & * & * & -\alpha I & 0 \\ * & * & * & * & -P' \end{bmatrix} < 0. \tag{41}$$

Box VIII

the system is linear and the uncertainty belongs to the polytopic class, it is sufficient to solve the LMIs at the vertices of the respective polyhedron [27], i.e., the set $\omega^{(k)}$; $k = 1, ..., n$, which can be defined through Eq. (14). $\square$

Remark 5. According to Corollary 1, the optimization problem to be solved now would be transformed into:

$$\min_{\mathcal{S}'} \text{ s.t. } (41), (42), (43); \quad k = 1, ..., n, \tag{44}$$

where $\mathcal{S}' \triangleq \{\alpha,\ P',\ Q',\ R',\ G,\ M\}$. The controller gain K can also be attained as $K = MG^{-1}$.

4. Simulation results and discussion

To verify the effectiveness of the proposed control approach, this section presents the simulation results. In order to take both free and contact motions into account, the human input is applied in two different cases:

- A unit step,
- A sine wave of the form $\sin(0.4\pi t)$.

4.1. Simulation results for certain system

In order to demonstrate the efficacy of the proposed L_1 controller, it was compared with Modified Sliding Mode (MSM) controller proposed by Park and Cho [28]. The architecture of the teleoperation system is identical for both controllers (depicted in Figure 1), except for the controller block (C_s). The corresponding control input for the MSM approach could be achieved through the following equation:

$$\begin{aligned} u(t) = {} & b_s \dot{x}_s(t) + k_s x(t) + y_z(t) \\ & - \frac{m_s}{m_m} \Big\{ b_m \dot{x}_m(t - d_m(t)) - F_h(t - d_m(t)) \\ & + y_z\left(t - d_m(t) - d_s(t - d_m(t))\right) \\ & + k_m x_m(t - d_m(t)) \Big\} - m_s \tilde{\lambda} \dot{\tilde{e}}(t) \\ & - K_{gain} \text{sat}\left(\frac{s_d(t)}{\tilde{\Phi}}\right), \end{aligned} \tag{45}$$

where $s_d(t) \triangleq \dot{\tilde{e}}(t) + \tilde{\lambda}\tilde{e}(t)$ is the sliding surface, $\tilde{e}(t) \triangleq -e(t)$ the opposite of the position error described before, $\tilde{\Phi}$ the thickness of the boundary layer to decrease the chattering phenomenon, K_{gain} a coefficient used to satisfy the sliding condition, and sat(.) the saturation function. All other parameters are the same as those given in the previous sections.

Since the parameter uncertainty is not considered in [28], the two aforementioned controllers were compared with the assumption of thoroughly known system dynamics. The results of the uncertain case for the L_1 controller will be then investigated in the next subsection.

The system parameters are summarized in Table 1. It should be noted that the dynamical properties of Phantom Omni haptic device were chosen for the local robot, as measured in [29], and the dynamical properties of Novint Falcon haptic device were selected for the remote robot based on the identification carried out in [30]. Zero initial conditions were also applied for master and slave robots in all simulations.

The environment was also simulated, the results of which revealed a viscoelastic characteristic in the compression mode with $k_z,\ b_z \neq 0$ and a pure elastic characteristic in the release mode with $k_z \neq 0,\ b_z = 0$.

The forward and backward time delays in this work are considered asymmetric and randomly time-varying with the corresponding bounds $\tilde{d}_m$ and $\tilde{d}_s$ mentioned in Table 1.

The corresponding parameters for the two con-

Table 1. System parameters [29,30].

Parameter	Value	Unit
k_m	6	N/m
b_m	17	Ns/m
m_m	0.2	kg
k_s	0	N/m
b_s	11	Ns/m
m_s	0.5	kg
ω_0	5	rad/s
k_z	3	N/m
b_z	3	Ns/m
$\tilde{d}_m$	1	s
$\tilde{d}_s$	1	s
$\tilde{\tau}_m$	0.2	–
$\tilde{\tau}_s$	0.2	–

Table 2. Parameters of controllers.

Parameter	Value	Unit
ω_0 (for L_1)	5	rad/s
ω_0 (for MSM)	0.8	rad/s
$\tilde{\lambda}$	5	1/s
$\tilde{\Phi}$	0.0004	–
K_{gain}	2	N

trollers are listed in Table 2. The tuning of the parameters regarding the MSM controller is carried out by trial and error such that the minimum possible steady-state error, as well as an acceptable control signal, will be obtained.

The suboptimal solution to the L_1 performance problem defined by Eq. (44) for $n = 1$ (i.e., no uncertainty) was found to be $\gamma = 0.0268$ at $\alpha = 0.026$ in free motion, $\gamma = 0.026$ at $\alpha = 0.016$ in the release mode, and $\gamma = 0.0294$ at $\alpha = 0.026$ in the compression mode by conducting a linear search on α and considering $||[\mathcal{S}', \gamma]||_2 < 10^9$. The corresponding state-feedback gain matrices were obtained as follows:

$$K_{free} = \begin{bmatrix} 5148 & 52 & -5223 & -141 & -10 & 82106 \end{bmatrix},$$

$$K_{release} = \begin{bmatrix} 6540 & 60 & -6590 & -170 & -10 & 101490 \end{bmatrix},$$

and:

$$K_{compression} =$$

$$\begin{bmatrix} 20660 & 220 & -20990 & -1150 & -20 & 216140 \end{bmatrix},$$

for free motion, the release contact, and compression contact modes, respectively.

Position tracking of the system by L_1 and MSM controllers subject to the unit step input is shown in Figure 2. It can be observed that although both controllers guarantee acceptable tracking, a position mismatch is found in the transient response of the MSM controller. It becomes more evident by taking a closer look at Figure 3, where the maximum overshoot of the MSM controller is nearly 6.5 times the L_1 controller, which further proves the significant superiority of the L_1 controller to its counterparts.

Figure 3 depicts the integral of position error which serves as the output of the L_1-based closed-loop system. One can easily figure out that the integral of position error is kept at a minimum by L_1 controller while it rises to approximately 17 times greater than that by MSM controller.

Another important fact is that the human force, not the position of the master robot, was considered as the exogenous input to the system in this paper. It thus implies that the same input force to the teleoperation system would not lead to the same master and, hence,

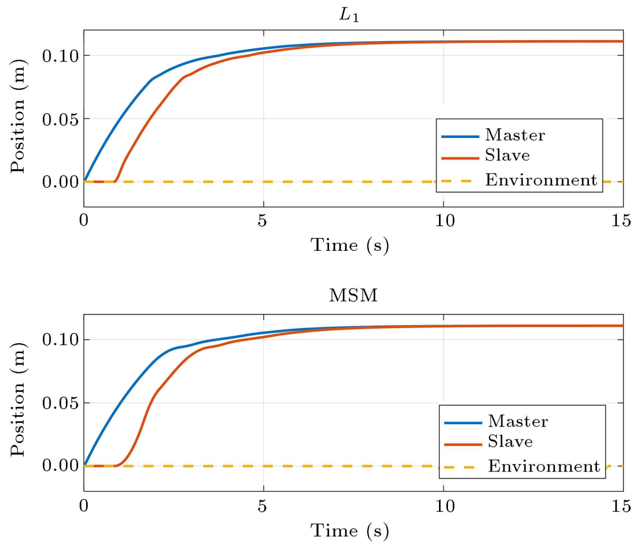

Figure 2. Master and slave positions for L_1 and MSM controllers in the case of unit step operator input.

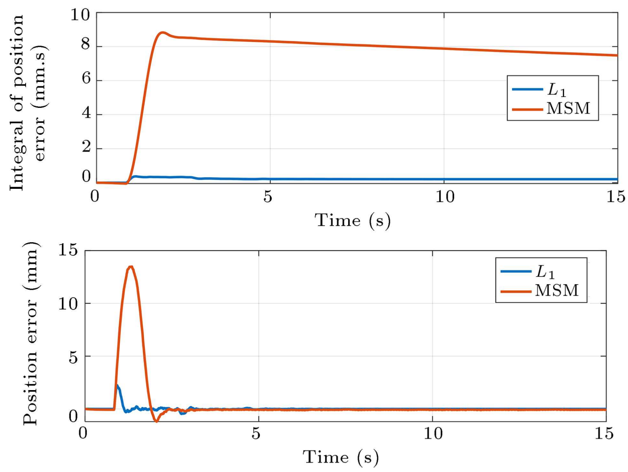

Figure 3. Position error and its integral for L_1 and MSM controllers in the case of unit step operator input. Note that the whole motion is in contact mode in this case. The depicted error for MSM is $-\tilde{e}(t)$.

slave movement due to inherently different controller structures. As observed in Figure 2, in spite of the same unit-step force inputs in both cases, a slight difference can be observed in the master positions that resulted from L_1 and MSM. However, this difference will not undermine the principal comparison. To be specific, the position error in each case is supposed to be determined by the master and slave movements in the same case. In this respect, Figure 3 represents a valid comparison between the synchronization errors.

Figure 4 shows the control input generated by each controller in the unit step case, as well. Despite its approximately same range, the L_1 control input exhibits smoother behavior; hence, it is preferable for a real experimental setup. More precisely, maintaining a low steady-state position error requires a constant con-

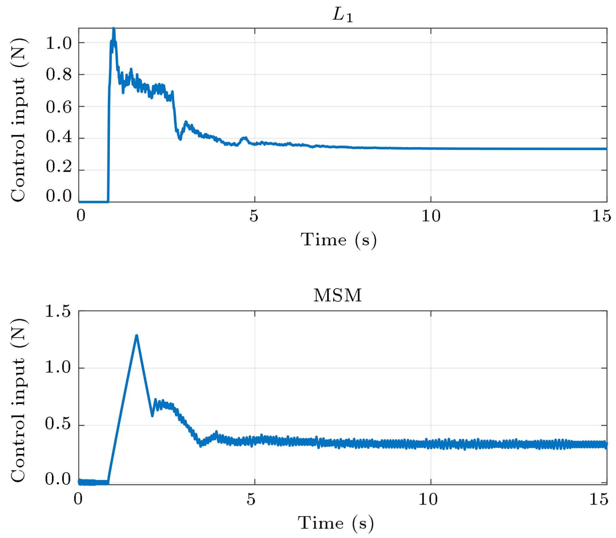

Figure 4. Control inputs for L_1 and MSM controllers in the case of unit step operator input.

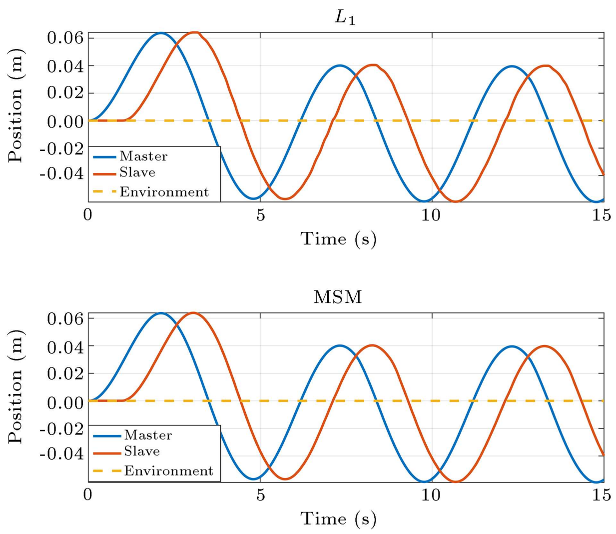

Figure 5. Master and slave positions for L_1 and MSM controllers in the case of sine wave operator input.

trol effort by means of L_1 while MSM imposes a more oscillatory actuator input in the same condition, which is undoubtedly detrimental to an actual experimental framework.

The same study was conducted for the two controllers in the case of sine wave as the human operator input. The quality of the position tracking resulting from this input is displayed in Figure 5 where both controllers exhibit almost a similar behavior. However, a comparison between the position error and its integral between both controllers was made, as shown in Figure 6, the results of which clearly showed the difference in this case.

Although the position error still lies in the same range for both controllers in Figure 6, the integral of position error is kept bounded by L_1 controller. It is,

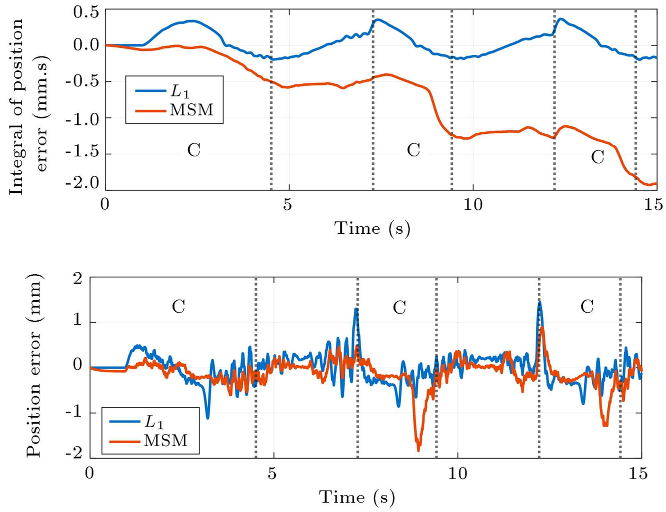

Figure 6. Position error and its integral for L_1 and MSM controllers in the case of sine wave operator input. The areas marked by 'C' are the intervals when the slave robot is in contact with the environment. Other areas are related to the free motion. The depicted error for MSM is $-\tilde{e}(t)$.

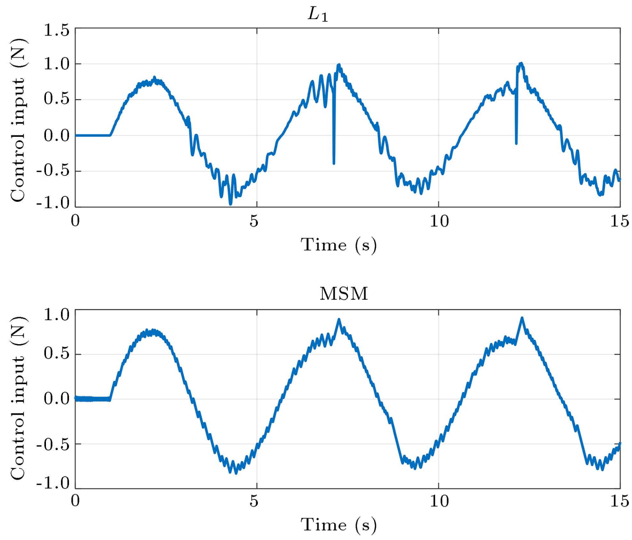

Figure 7. Control inputs for L_1 and MSM controllers in the case of sine wave operator input.

however, not the case for MSM controller whereby the integral of error keeps growing unboundedly, especially during contact intervals. This result was obtained mainly because the L_1-based scheme directly took the infinity-norm of the integral of position error under control as its output.

The generated control inputs are also presented in Figure 7. Compared to the step input, the signals are more similar in this case, excluding the high-frequency oscillations that are relatively more apparent in the MSM controller.

From the results of this subsection, it can be concluded that the L_1 controller is able to provide the asymmetrically delayed teleoperation system with a promising response from the maximum overshoot perspective while maintaining a low steady-state position error.

4.2. Simulation results for uncertain system

The performance results of the L_1 controller for the teleoperation system containing parametric uncertainties are presented in this subsection.

The uncertain parameters are listed in Table 3 where δ_{mm}, δ_{ms}, δ_{bm}, and δ_{bs} denote the uncertainty of the corresponding parameters that are set such that the uncertain matrices A_m and A_s both become in the form:

$$\begin{bmatrix} 0 & 1 \\ -k_i(\rho)/m_i(\rho) & -b_i(\rho)/m_i(\rho)+\delta \end{bmatrix}, \quad i=\{m,s\},$$

where $-2 \le \delta \le 2$. Therefore, the polytopic domain of the uncertain system contains $n=2$ vertices. All other corresponding parameters are the same as those given in Tables 1 and 2. The suboptimal solution to the L_1 performance problem defined by Eq. (44) was found to be $\gamma = 0.0452$ at $\alpha = 0.043$ in the free motion, $\gamma = 0.0465$ at $\alpha = 0.046$ in the release mode, and $\gamma = 0.0288$ at $\alpha = 0.024$ in the compression mode by conducting a linear search on and considering $||[\mathcal{S}', \gamma]||_2 < 10^9$. The corresponding state-feedback gain matrices were obtained as follows:

$$K_{free} = \begin{bmatrix} 1762 & 20 & -1808 & -62 & -7 & 17499 \end{bmatrix},$$

$$K_{release} = \begin{bmatrix} 1684 & 16 & -1709 & -61 & -7 & 15795 \end{bmatrix},$$

and:

$$K_{compression} = \begin{bmatrix} 72.03 & 0.74 & -73.40 & -4.86 & -0.05 & 501.20 \end{bmatrix} \times (10^3),$$

for the free motion, release contact mode, and compression contact mode, respectively.

In order to avoid repetitive results, the figures regarding only the master-slave positions and errors are provided here. From Figures 8–11, it can be deduced that despite the parameter uncertainties, the synchronization quality of the L_1 controller is not degraded, and relatively small overshoots would result

Table 3. Uncertain system parameters.

Parameter	Value	Unit
b_m	$17+\delta_{bm}$	Ns/m
m_m	$0.2+\delta_{mm}$	kg
b_s	$11+\delta_{bs}$	Ns/m
m_s	$0.5+\delta_{ms}$	kg

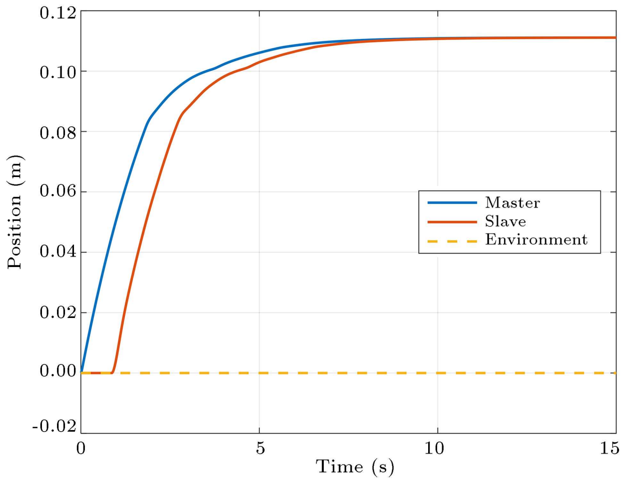

Figure 8. Master and slave positions in the case of unit step operator input using L_1 controller for uncertain system.

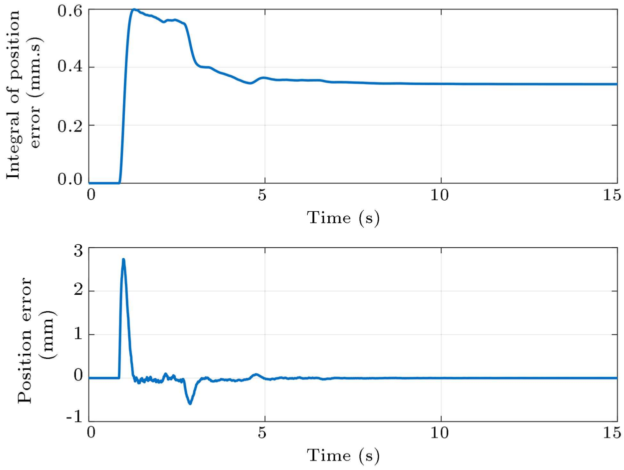

Figure 9. Position error and its integral in the case of unit step operator input using L_1 controller for uncertain system. Note that the whole motion is in contact mode in this case.

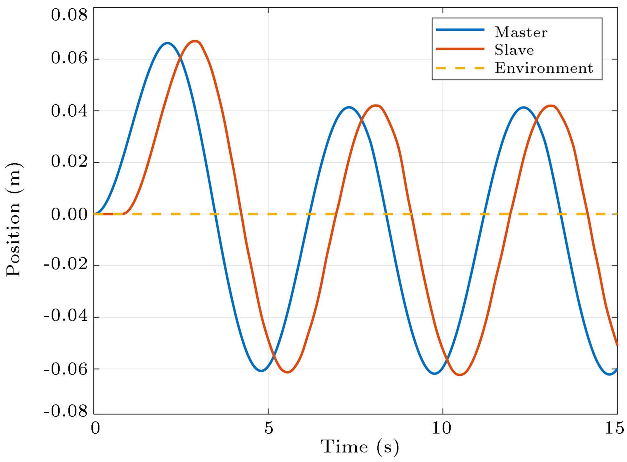

Figure 10. Master and slave positions in the case of sine wave operator input using L_1 controller for uncertain system.

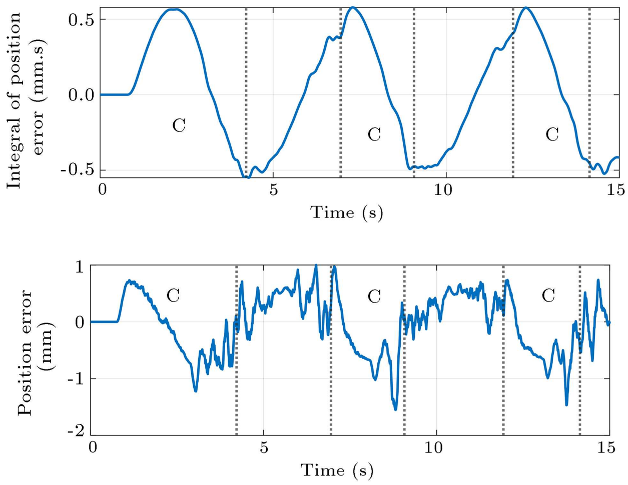

Figure 11. Position error and its integral in the case of sine wave operator input using L_1 controller for uncertain system. The areas marked by 'C' are the intervals when the slave robot is in contact with the environment. Other areas are related to the free motion.

from both step and sine inputs. The integral of the position error is also shown to be kept bounded in line with theory and previous results.

The only issue that might be raised here is the larger value of γ in the uncertain case, compared to the certain case. This problem indicates that widening the domain of the uncertainty could possibly lead to a more significant L_1 gain which, in turn, would risk the chance of finding the optimal or suboptimal solution to Problem (44) as $\gamma \to \infty$. In fact, in case the optimization problem does not have a positive real solution, the proposed L_1 controller fails to provide a controller for the teleoperation system, which can be considered as a drawback compared to some other control approaches such as sliding mode. However, as long as a solution exists for the aforementioned optimization problem, the L_1-based controller demonstrates a promising position synchronization capability according to the results presented in this section.

5. Conclusion and future directions

An L_1-based control architecture was proposed in this study for a one-Degree-od-Freedom (one-DoF) teleoperation system with randomly varying time delays and polytopic uncertainty. The controller was designed through the Linear Matrix Inequality (LMI) approach, considering the concept of quadratic stability.

Simulation results showed that by incorporating this controller into the teleoperation system, good position tracking by the remote robot could be attained while preserving the haptic feedback to the local side. Comparing the position tracking resulting from the L_1-based controller with the modified sliding mode controller demonstrated a promising response of the proposed control approach from the maximum overshoot point of view. It was also shown that the application of the proposed L_1 controller could result in low steady-state error.

Since the controller is designed for linear single-DoF teleoperation, its application is thus limited to such systems. Most real teleoperation systems incorporate nonlinear multi-DoF manipulators that require a more complicated design. Another limitation of the current work is the assumption of viscoelastic environment, which may not be applicable to all circumstances.

As a future work, we intend to implement the proposed control framework on a real setup. Of note, another improvement could be made by designing an L_1 controller based on nonlinear systems.

Nomenclature

Symbols

b	Damping coefficient
d	Time delay
k	Stiffness
K	Gain matrix
m	Mass
t	Time
u	Control input
w	External disturbance
x	Position
$\dot{x}$	Velocity
y	Output
z	Performance output
$*$	Symmetric element

Greek symbols

γ	Noise attenuation level
ρ	Uncertainty domain parameter
ω_0	Cut-off frequency

Subscripts

e	Error
f	Filter
m	Master side
s	Slave side
z	Environment

Operators

$\lambda(.)$	Eigenvalue
$\|\|.\|\|_n$	n-norm

References

1. Meshram, D.A. and Patil, D.D. "5G enabled tactile internet for tele-robotic surgery", *Procedia Computer Science,* **171**, pp. 2618–2625 (2020).

2. Kebria, P.M., Abdi, H., Dalvand, M.M., et al. "Control methods for internet-based teleoperation systems: A review", *IEEE Transactions on Human-Machine Systems,* **49**(1), pp. 32–46 (2018).

3. Tabatabaei, S.H., Zaeri, A.H., and Vahedi, M. "Design an impedance control strategy for a teleoperation system to perform drilling process during spinal surgery", *Transactions of the Institute of Measurement and Control*, **41**(10), pp. 2947–2956 (2019).

4. Ji, P., Ma, F., and Min, F. "Terminal traction control of teleoperation manipulator with random jitter disturbance based on active disturbance rejection sliding mode control", *IEEE Access*, **8**, pp. 220246–220262 (2020).

5. Chan, L., Naghdy, F., and Stirling, D. "Application of adaptive controllers in teleoperation systems: A survey", *IEEE Transactions on Human-Machine Systems*, **44**(3), pp. 337–352 (2014).

6. Hosseini-Suny, K., Momeni, H., and Janabi-Sharifi, F. "Model reference adaptive control design for a teleoperation system with output prediction", *Journal of Intelligent & Robotic Systems*, **59**(3–4), pp. 319–339 (2010).

7. Namnabat, M., Zaeri, A., and Vahedi, M. "A passivity-based control strategy for nonlinear bilateral teleoperation employing estimated external forces", *Journal of the Brazilian Society of Mechanical Sciences and Engineering*, **42**(12), pp. 1–10 (2020).

8. Franco, E. "Combined adaptive and predictive control for a teleoperation system with force disturbance and input delay", *Frontiers in Robotics and AI*, **3**, p. 48 (2016).

9. Uddin, R. and Ryu, J. "Predictive control approaches for bilateral teleoperation", *Annual Reviews in Control*, **42**, pp. 82–99 (2016).

10. Yazdankhoo, B. and Beigzadeh, B. "Increasing stability in model-mediated teleoperation approach by reducing model jump effect", *Scientia Iranica,* **26***(Special Issue on: Socio-Cognitive Engineering)*, pp. 3–14 (2019).

11. Yazdankhoo, B., Nikpour, M., Beigzadeh, B., et al. "Improvement of operator position prediction in teleoperation systems with time delay: Simulation and experimental studies on phantom omni devices", *JJMIE*, **13**(3), pp. 197–205 (2019).

12. Nikpour, M., Yazdankhoo, B., Beigzadeh, B., et al. "Adaptive online prediction of operator position in teleoperation with unknown time-varying delay: simulation and experiments", *Neural Computing and Applications*, **33**(13), pp. 7575–7592 (2021).

13. Shokri-Ghaleh, H. and Alfi, A. "Bilateral control of uncertain telerobotic systems using iterative learning control: Design and stability analysis", *Acta Astronautica*, **156**, pp. 58–69 (2019).

14. Gormus, B., Yazici, H., and Kucukdemiral, I.B. "Robust H-infinity control of an uncertain bilateral teleoperation system using dilated LMIs", *Transactions of the Institute of Measurement and Control*, **44**(6), pp. 1275–1287 (2022).

15. Bavili, R.E., Bavil, A.F., and Akbari, A. "Control of a bilateral teleoperation system in the presence of varying time delay, model uncertainty and actuator faults", *International Journal of Dynamics and Control*, **9**, pp. 1261–1276 (2021).

16. Kang, J.S., Lee, M.C., and Yoon, S.M. "Bilateral control based rupture protection method in surgical robot using improved master device", *International Journal of Control, Automation and Systems*, **14**(4), pp. 1073–1080 (2016).

17. Li, Y., Liu, Z., Wang, Z., et al. "Adaptive control of teleoperation systems with prescribed tracking performance: a BLF-based approach", *International Journal of Control*, **95**(6), pp. 1600–1610 (2020).

18. Vidyasagar, M. "Optimal rejection of persistent bounded disturbances", *IEEE Transactions on Automatic Control*, **31**(6), pp. 527–534 (1986).

19. Blanchini, F. and Sznaier, M. "Rational L_1 suboptimal compensators for continuous-time systems", *IEEE Transactions on Automatic Control*, **39**(7), pp. 1487–1492 (1994).

20. Zhu, J. and Chen, J. "Stability of systems with time-varying delays: An L_1 small-gain perspective", *Automatica*, **52**, pp. 260–265 (2015).

21. Li, Y., Lam, J., and Luo, X. "Convex optimization approaches to robust L_1 fixed-order filtering for polytopic systems with multiple delays", *Circuits, Systems & Signal Processing*, **27**(1), pp. 1–22 (2008).

22. Li, Y. and Liang, Y. "Gain-scheduled L-one control for linear parameter-varying systems with parameter-dependent delays", *Journal of Control Theory and Applications*, **9**(4), pp. 617–623 (2011).

23. Maiti, R., Sharma, K.D., Sarkar, G., et al. "Modelling and control of delayed, nonlinear, uncertain, disturbed air heater employing fuzzy PDC-L_1 adaptive scheme", *IEEE Transactions on Industrial Electronics*, **68**(11), pp. 11328–11338 (2021).

24. Nguyen, K.-D. and Dankowicz, H. "Delay robustness and compensation in L_1 adaptive control", *Procedia IUTAM*, **22**, pp. 10–15 (2017).

25. Sadeghi, M.S., Momeni, H.R., and Amirifar, R. "H_∞ and L_1 control of a teleoperation system via LMIs", *Applied Mathematics and Computation*, **206**(2), pp. 669–677 (2008).

26. Hua, C.-C. and Liu, X.P. "Delay-dependent stability criteria of teleoperation systems with asymmetric time-varying delays", *IEEE Transactions on Robotics*, **26**(5), pp. 925–932 (2010).
27. Gu, K., Chen, J., and Kharitonov, V.L., *Stability of Time-Delay Systems*, Springer Science & Business Media (2003).
28. Park, J.H. and Cho, H.C. "Sliding mode control of bilateral teleoperation systems with force-reflection on the internet", *IEEE/RSJ International Conference on Intelligent Robots and Systems (IROS 2000)*, **2**, pp. 1187–1192 (2000).
29. Hilliard, T. and Pan, Y.-J. "Stabilization of asymmetric bilateral teleoperation systems for haptic devices with time-varying delays", *American Control Conference*, pp. 4538–4543 (2013).
30. Khadivar, F., Sadeghnejad, S., Moradi, H., et al. "Dynamic characterization of a parallel haptic device for application as an actuator in a surgery simulator", *2017 5th RSI International Conference on Robotics and Mechatronics (ICRoM)*, pp. 186–191 (2017).

Biographies

Behnam Yazdankhoo received his BSc degree in Mechanical Engineering from Amirkabir University of Technology, Tehran, Iran in 2015 and his MSc degree in Biomedical Engineering (Biomechanics) from Iran University of Science and Technology, Tehran, Iran in 2018. He is currently pursuing his PhD degree in Mechanical Engineering at University of Tehran, Tehran, Iran. His research interests are control of robotic/telerobotic systems and application of the artificial intelligence therein.

Farshid Najafi received his BSc degree in Mechanical Engineering from Sharif University of Technology, Tehran, Iran in 1996 and his MSc and PhD degrees in Mechanical Engineering from University of Manitoba, Manitoba, Canada in 2003 and 2009, respectively. He then joined the School of Mechanical Engineering at University of Tehran, Tehran, Iran where he is currently an Assistant Professor. His main research interests include medical robots, mechatronics, biomechatronics, and haptic devices.

Mohammad Reza Ha'iri Yazdi received his BSc and MSc degrees in Mechanical Engineering from Amirkabir University of Technology, Tehran, Iran in 1985 and 1987, respectively. He received his PhD degree from Imperial College London in 1992 and since then, he has worked at University of Tehran, Tehran, Iran as a Professor at School of Mechanical Engineering. His main research interests include design, simulation, manufacturing, and control of dynamic systems.

Borhan Beigzadeh received his PhD degree in Mechanical Engineering from Sharif University of Technology in 2011. He has been working on dynamic walking systems and studying their correlation with dynamic passive/active manipulation systems. He then joined Iran University of Science and Technology, Tehran, Iran where he is currently an Associate Professor at School of Mechanical Engineering, and established Biomechatronics and Cognitive Engineering Research Laboratory. His research interests cover non-linear dynamics and control, robotics, biomechatronics, and cognitive engineering.